

Quantum Walks via Quantum Cellular Automata

Pedro C.S. Costa,¹ Renato Portugal,² and Fernando de Melo¹

¹*Brazilian Center for Research in Physics-CBPF, Rua Dr. Xavier Sigaud, 150 - Urca - Rio de Janeiro - RJ - Brasil*

²*National Laboratory of Scientific Computing-LNCC, Av. Getúlio Vargas, 333 - Quitandinha, Petrópolis - RJ- Brasil*

(Dated: March 16, 2022)

Very much as its classical counterpart, quantum cellular automata are expected to be a great tool for simulating complex quantum systems. Here we introduce a partitioned model of quantum cellular automata and show how it can simulate, with the same amount of resources (in terms of effective Hilbert space dimension), various models of quantum walks. All the algorithms developed within quantum walk models are thus directly inherited by the quantum cellular automata. The latter, however, has its structure based on local interactions between qubits, and as such it can be more suitable for present (and future) experimental implementations.

I. INTRODUCTION

Random walks, a certain type of stochastic processes, were introduced at the beginning of the twentieth century [1]. Since then, random walks have turned into a powerful tool and found applications in areas as diverse as economics [2], ecology [3], computer science [4], and physics [5, 6]. Quantum mechanics was developed roughly at the same time. However, it took almost 90 years for the quantum version of random walks, nowadays known as *quantum walks* (QWs) to be proposed [7]. Despite of its relative young age, the quantum counterpart of random walks is also being employed in various applications, most notably in quantum simulations [8, 9] and in quantum algorithms [10]. Quantum walks, like its predecessor, comes in various flavors – coined [7], Szegedy [39], staggered [11], and staggered with Hamiltonians [12], to cite a few – each with its own specificity and tuned to better deal with a given problem at hand. Foremost, some models of quantum walks were shown to form a universal platform for quantum computation [13, 14]. All this versatility and possible applications prompted an intense experimental activity with various realizations of quantum walks, for instance trapped ions [15], optical lattices [16] and more [17].

Most of quantum walk models, however, suffer from two major implementation drawbacks: *i)* the space associated to the walkers position is usually large, and as such it requires a high dimensional quantum system to encode it. *ii)* The unitary evolving the walker is a global one, being applied in all the space in every step. These two points together tremendously limit the size of experimental implementations, and fundamentally put the promising advantages of quantum walks into the far future.

On the classical world, the computational model of *Cellular Automata* (CA) is also largely employed [18]. Cellular automata are abstract dynamical/computational systems with discrete space and time. The space consists of a d -dimensional network of cells. At each time step

individual cells assume one state from a finite number of possible states. The evolution of the network is given in parallel at discrete time steps: at each time t , the state of each cell depends only on the state of its neighboring cells at time $t - 1$ through a local update rule [19]. Classical cellular automata, first proposed by John von Neumann and Stanislaw Ulam [20], are used in applications ranging from cryptography [21] up to the simulation of fluid dynamics [22], and the description of biological systems [23].

Despite of all the results for classical cellular automata, its quantum counterpart, the quantum cellular automata (QCA), does not share the same amount of research activity. The phenomenology and applications of quantum cellular automata are very scarce. One possible reason for the QCA to not be yet widely employed is that a clear definition, that inherits the main qualities of classical CAs while allowing for a more powerful quantum processing, was not available until recently. The idea of quantum cellular automata was first pursued by Gröss and Zeilinger [24], with a model that later proved to not abide by the locality constraint expected of cellular automata [25]. After this first tentative various models of quantum cellular automata were put forward [26]. After a period of discussion about the proper quantization of cellular automata, in recent years an agreement was obtained and many of the definitions were proved equivalent [27].

The main goal of this contribution is to start exploring the model of quantum cellular automata, as a suitable platform for quantum algorithms. We do so by showing that various models of quantum walks can be translated to a quantum cellular automata dynamics using the same amount of resources (effective Hilbert space dimension). More concretely we show how to implement two models of QWs – namely, the coined and the staggered QW with Hamiltonians, which are known to encompass a large class of QW models [12] – within the partitioned QCA model (defined below). Quantum cellular automata, besides employing qubits – which are the

base of most quantum computers architectures [28–30] – they do not suffer from the above mentioned drawbacks present in QWs: interactions in QCA are local and translation invariant (both in space and time). These QCA advantages, when combined with the various algorithms developed for QWs, might render the implementation of large quantum algorithms viable to current technology.

The article is organized as follows: In Section II we present the QCA formal definition and work with some examples. Moving forward in Section III we show how to translate the QWs formalism to the QCA. We begin with the coined model, starting with a concrete example in the one dimensional lattice, establishing the motion equation in both quantum models of computation to see that they indeed give to us the same dynamics time by time. Then, afterwards we move to the general recipe. Following the same previous steps we do the same for the staggered quantum walk with Hamiltonian (SQWH). Finally in Section IV we state some final considerations with possibles advantages and applications for these translations.

II. QUANTUM CELLULAR AUTOMATA: DEFINITION AND EXAMPLES

In classical cellular automata (think for instance on the Wolfram’s elementary CA [19]), the evolution of the cell at position x is given in two steps: i) First the state of the neighboring cells of x is read. ii) Second, conditioned on this first read measurement, the state of the cell x is updated according to a fixed local rule. This is then repeated for all the cells in the automata in a translation invariant way, i.e., using the same updating rule for all cells and without a specific updating ordering. The locality of the automata is guaranteed by the neighboring scheme \mathcal{N} which states that only the cells in the set $\mathcal{N}_x = \mathcal{N} + x$ will influence the update of cell at position x .

This idea of cellular automata clearly can not be directly translated to the quantum realm: the state of quantum systems cannot be read without disturbing the system’s state. Moreover, the possible non-commutativity of quantum operations imposes some constraints on the translation invariant update. Ultimately, the challenges to properly define a quantum cellular automata are rooted at the impossibility of cloning quantum states [31]. Besides that, the classical automata dynamics may be irreversible, which is in contrast with a unitary quantum evolution. One way to define reversible automata is by employing the Margolus block scheme [32]. Here we define a Partitioned Unitary Quantum Cellular Automata (PUQCA) combining the Margolus block scheme, the unitary aspects of the QCA introduced by Pérez-Delgado and Donny Cheung [33], and some dynamical attributes

present in the QCA initiated by Watrous [34]. This combination makes clear the locality and translation invariance properties, besides giving a direct quantum generalization of classical partitioned cellular automata.

Two features will become central to our definition of partitioned quantum cellular automata: First each cell is to be divided into n subcells. This subdivision of each cell generates a finer description for the space where the automaton is defined – be it a lattice or the more general case of a graph. Second, we will employ different tilings over this finer description of the space. Each tiling covers the full space, with an individual tile covering a finite subset of the subcells. The tiling is then a uniform partition of the set of subcells, with each tile an element of this partition.

With these elements, we are in position to define our partitioned unitary quantum cellular automata.

Definition 1 (PUQCA). *A Partitioned Unitary Quantum Cellular Automata is a 5-tuple $(L, \mathcal{N}, \Sigma, \{\mathcal{T}_i\}, \{W_i\})$ consisting of:*

1. *a d -dimensional lattice of cells indexed by integers $L = \mathbb{Z}^d$;*
2. *a finite neighborhood scheme $\mathcal{N} \subseteq L$;*
3. *a finite set Σ of orthogonal basis states with $\mathcal{H}_\Sigma = \text{span}\{|\sigma\rangle_{\sigma \in \Sigma}\}$. Each cell is divided in n subcells, and to the i -th subcell we assign a copy \mathcal{H}_{Σ_i} of \mathcal{H}_Σ . The total space associated to each cell is then $\mathcal{H}_\Xi = \bigotimes_{i \in \{0, \dots, n-1\}} \mathcal{H}_{\Sigma_i}$;*
4. *a finite set of tilings $\{\mathcal{T}_i\}_{i=0}^{N-1}$. Each tiling is the union of identical non-overlapping tiles, $\mathcal{T}_i = \bigcup_j T_j^{(i)}$, with each tile $T_j^{(i)}$ containing only subcells of neighboring cells.*
5. *a set of local unitary functions $\{W_i\}_{i=0}^{N-1}$. The same unitary W_i is applied to each tile $T_j^{(i)}$ of the tiling \mathcal{T}_i ;*

With this definition, the transition function $\mathcal{E} : (\mathcal{H}_\Xi)^{\otimes L} \mapsto (\mathcal{H}_\Xi)^{\otimes L}$, which updates the automaton state from the time t to $t + 1$, is the given by

$$\mathcal{E} = \prod_{i=0}^{N-1} \left(\bigotimes_{T_j^{(i)} \in \mathcal{T}_i} W_i \right). \quad (1)$$

To work with these tilings more precisely, it is convenient put labels in each subcell. Given the cell at position $i \in L$, its subcells are denoted by i_j , with $j \in \{0, \dots, n-1\}$. For instance, suppose we have an one-dimensional

lattice where each cell has two subcells, and the neighbor scheme is $\mathcal{N}_i = \{i-1, i, i+1\}$. In this case two tilings are sufficient to evolve the automaton: The first tiling is given by $\mathcal{T}_0 = \bigcup_{i \in \mathbb{Z}} T_i^{(0)}$ with each tile defined as $T_i^{(0)} = \{i_0, i_1\}$. For the second tiling, $\mathcal{T}_1 = \bigcup_{i \in \mathbb{Z}} T_i^{(1)}$, each tile is given by $T_i^{(1)} = \{i_1, (i+1)_0\}$. It is then clear that the first tiling is responsible for “reading” the state of each cell, while the second one is responsible for the interaction between the neighboring cells – resembling the unitary quantum cellular automata defined in [33]. Now that the tilings’ structure is established, the action of the unitary functions is apparent:

$$\begin{aligned} W_0 : (\mathcal{H}_{\Sigma_0})_i \otimes (\mathcal{H}_{\Sigma_1})_i &\rightarrow (\mathcal{H}_{\Sigma_0})_i \otimes (\mathcal{H}_{\Sigma_1})_i \\ W_1 : (\mathcal{H}_{\Sigma_1})_i \otimes (\mathcal{H}_{\Sigma_0})_{i+1} &\rightarrow (\mathcal{H}_{\Sigma_1})_i \otimes (\mathcal{H}_{\Sigma_0})_{i+1}, \end{aligned}$$

for all $i \in \mathbb{Z}$. Therefore, in this example we can explicit our transition function as

$$\mathcal{E} = \left(\bigotimes_{T_i^{(1)} \in \mathcal{T}_1} W_1 \right) \left(\bigotimes_{T_i^{(0)} \in \mathcal{T}_0} W_0 \right). \quad (2)$$

All this construction can be apprehended from Fig.(1-a).

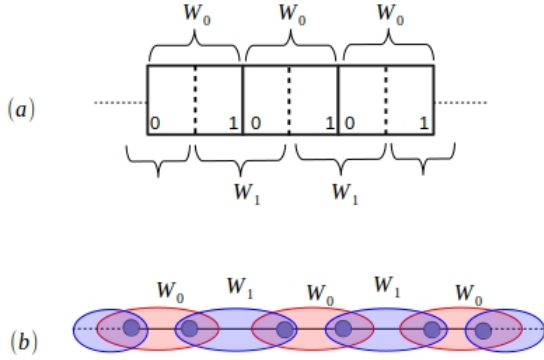


FIG. 1. **1-dimensional automaton.** In top-panel (a) it is shown how each cell is split in two subcells, and how the unitary operators W_i are applied in accordance with the two tilings. In the bottom-panel (b) it is shown the same 1-d automaton, but now in the graph perspective. The tiling \mathcal{T}_0 is represented by the red ellipses, while the tiling \mathcal{T}_1 is shown in blue.

The above definition of the PUQCA immediately generalizes to QCA over a regular graph $G = G(V, E)$. In this situation, the neighborhood scheme is represented by the edge set E , and the tilings are defined over partitions of the graph G into complete subgraphs – in every tiling all the vertices are included, and the union of

the tilings must contain all the edges. Within graph theory, tilings are usually called tessellations (see the definitions used III B below). We also can see how the one-dimensional example is represented by the “graph perspective” in Fig.(1-b). Another example of a QCA in the graph picture is shown in Fig. (2).

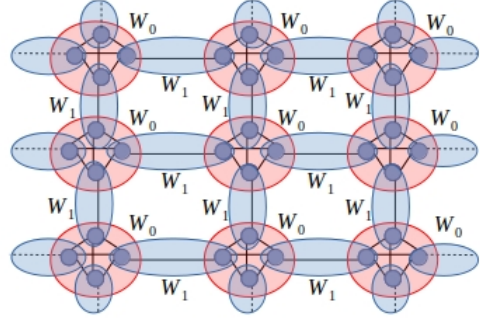


FIG. 2. **Graph perspective: 2-dimensional automaton.** For the automaton defined over the 2-dimensional lattice, with four neighbors, each cell is transformed into a complete graph with 4 vertices (K4). The first tiling is shown in red, with corresponding unitary operation W_0 acting only on the subcells of each cell. The second tiling is depicted in blue, with the unitary operation W_1 being responsible for the interaction between neighboring cells.

In what follows we will mostly employ the graph perspective, as it makes clear the translation procedures from quantum walks to quantum cellular automata.

III. TRANSLATING QUANTUM WALKS INTO QUANTUM CELLULAR AUTOMATA

This section contains our main result: how to translate a large class of quantum walk models into quantum cellular automata models. We focus on the Coined Quantum Walk over a d -regular graph (CQW_d) and on the Staggered Quantum Walk with Hamiltonians (SQWH), as these two models were already shown to encompass various models of quantum walks [12]. The amount of resources in the quantum walk is compared to the correspondent quantum cellular automaton.

A. CQW_d \subseteq QCA

1. Coined quantum walk over a d -regular graph.

Coined quantum walks were the first to be devised [7], likely due to their similarity to the classical case. The main difference from the classical to the quantum walk lies in the possibility, in the latter, of superpositions of the coin values and walker positions. Since these early times, the definition of quantum walks evolved, specially to cope with general dynamics in arbitrary finite graphs [35]. Given a graph $G = G(V, E)$ its vertices are associated to the walker's classical positions, while its edges define the possible directions the walker can take in a single step. To the position $i \in V$ and direction $(i, j) \in E$ we associate the state $|(i, j), i\rangle$. Defining \mathcal{N}_i^G as the graph-neighborhood of a vertex i , $\mathcal{N}_i^G = \{j | (i, j) \in E\}$, the total Hilbert space associated to the quantum walk is given by

$$\mathcal{H}_G = \text{span}(\{|(i, j), i\rangle | (i, j) \in E, i \in V, j \in \mathcal{N}_i^G\}).$$

As each edge is connected to exactly two vertices, the dimension of \mathcal{H}_G is $2|E|$ [36].

The dynamics of a quantum walker is given by first the “flip” of a quantum coin, followed by a coin-dependent coherent displacement. Given a walker in the state $|(i, j), i\rangle$, the coin operator must create a superposition of all allowed directions, i.e., a superposition of the states $|(i, k), i\rangle$ for all $k \in \mathcal{N}_i^G$. The action of the coin operator is more easily understood if we decompose \mathcal{H}_G in blocks related to each vertex: $\mathcal{H}_G = \oplus_{i \in V} \mathcal{H}_G^{(i)}$, with $\mathcal{H}_G^{(i)} = \text{span}(\{|(i, j), i\rangle | (i, j) \in E, j \in \mathcal{N}_i^G\})$. For a d -regular graph, each such a block is a d -dimensional Hilbert space. The action of the coin operator $C : \mathcal{H}_G \rightarrow \mathcal{H}_G$ can be written as:

$$C = \bigoplus_{i \in V} C_i, \quad (3)$$

where each C_i is a unitary acting on $\mathcal{H}_G^{(i)}$. If the coin flip is independent of the vertex, which is usually the case, we take the action of the coin operator to be identical in each vertex-subspace. To finish the walker step we must define the shift operator $S_\pi : \mathcal{H}_G \rightarrow \mathcal{H}_G$. As the walker can only walk “over” the edges, the action of the most general shift operator is given by:

$$S_\pi |(i, j), i\rangle = |(\pi(i), j), j\rangle, \forall i \in V \text{ and } \forall (i, j) \in E. \quad (4)$$

Here π is a permutation that fixes the walker's direction after the step, i.e., π is a permutation between the d neighbors of the receiving vertex such that $\pi(i) \in \mathcal{N}_j^G$. As the permutation π fully determines the shift operator, in a d -regular graph there are only $d!$ different shift

operators. Moreover, since this permutation does not change the vertex value, we can choose the identity permutation and absorb some possible relabeling in the coin operator. The shift for which we take the identity permutation, $S_I |(i, j), i\rangle = |(i, j), j\rangle$, is known as the flip-flop, given that $S_I^2 = \mathbb{I}$. Given all that, the one time step evolution of the quantum walker is given by the unitary $U_G : \mathcal{H}_G \rightarrow \mathcal{H}_G$, whose action can be written as:

$$U_G = S_I \cdot C. \quad (5)$$

In what follows we show how to translate each element of the coined quantum walk into a quantum cellular automata description. We start with a simple example, followed by a general translation procedure.

2. One dimensional example.

The most paradigmatic example of coined quantum walk is the one-dimensional case, with a two-states coin. This construction closely resembles the classical random walk, and it was the main inspiration for the generalization to the quantum domain [7]. In this instance the walk happens in a one-dimensional lattice, which can be seen as a infinite 2-regular graph. In such a graph perspective, the set of vertices is $V = \mathbb{Z}$, and the set of edges is $E = \{(i, i+1) | i \in V\}$, leading to a vertex-neighborhood $\mathcal{N}_i^G = \{i-1, i+1\}$. Moreover, if the walker is on the vertex i moving to the right we associate to it the state $|(i, i+1), i\rangle$, while if it is moving to the left we describe it by the state $|(i, i-1), i\rangle$. For the walker in such a position, the coin operator must superpose the two directions of movement, $|(i, i+1), i\rangle$ and $|(i, i-1), i\rangle$. This can be done by choosing $C_i : \mathcal{H}_G^{(i)} \rightarrow \mathcal{H}_G^{(i)}$ as a SU(2) operator

$$C_i = \begin{pmatrix} q & p \\ p & q \end{pmatrix} \forall i \in V,$$

with $p, q \in \mathbb{C}$ respecting the unitarity constraints $|p|^2 + |q|^2 = 1$ and $p^*q + q^*p = 0$. The total coin operator is then $C = \bigoplus_{i \in V} C_i$. Traditionally, the shift operator does not change the coin value, i.e., it keeps the direction of the movement. This shift is known as the “moving” operator, and it acts on \mathcal{H}_G as follows:

$$\begin{aligned} S_X |(i, i-1), i\rangle &= |(i-2, i-1), i-1\rangle, \\ S_X |(i, i+1), i\rangle &= |(i+2, i+1), i+1\rangle. \end{aligned} \quad (6)$$

The relation of between the moving shift S_X to the flip-flop S_I one is simple: $S_X = X \cdot S_I$, where $X = \bigoplus_{i \in V} X_i$ with

$$X_i = \begin{pmatrix} 0 & 1 \\ 1 & 0 \end{pmatrix} \forall i \in V.$$

A single step evolution is then given by $U = X \cdot S_I \cdot C$ [37]. If the state of the system at time t is

$$|\psi(t)\rangle = \sum_{i \in V} \left(\psi_{(i,i-1)}(i,t) |(i,i-1),i\rangle + \psi_{(i,i+1)}(i,t) |(i,i+1),i\rangle \right),$$

where $\psi_{(i,j)}(i,t) := \langle (i,j),i | \psi(t) \rangle$ is the amplitude of the walker being located at the vertex i pointing to the vertex j at time t . Then the state at $t+1$ is obtained by $U|\psi(t)\rangle$, which gives

$$\sum_{i \in V} \left[(q\psi_{(i,i-1)}(i,t) + p\psi_{(i,i+1)}(i,t)) |(i-2,i-1),i-1\rangle + (p\psi_{(i,i-1)}(i,t) + q\psi_{(i,i+1)}(i,t)) |(i+2,i+1),i+1\rangle \right].$$

It is now immediate to obtain the recurrence relations that govern the quantum walk dynamics:

$$\begin{aligned} \psi_{(i-2,i-1)}(i-1,t+1) &= q\psi_{(i,i-1)}(i,t) + p\psi_{(i,i+1)}(i,t), \\ \psi_{(i+2,i+1)}(i+1,t+1) &= p\psi_{(i,i-1)}(i,t) + q\psi_{(i,i+1)}(i,t). \end{aligned}$$

These are the dynamical equations that fully describe the walker dynamics in one dimensional lattice with a moving shift.

Now we want to reproduce the dynamics achieved above within the cellular automata formalism. In order to do that, each vertex $i \in V$ we change to a cellular automaton cell. As each vertex has two neighbors (leading to a two-dimensional coin), each automaton cell is divided into two sub-cells. A cell i is then composed by two sub-cells labeled by $(i)_{(i-1)}$ and $(i)_{(i+1)}$. In each subcell we place a two-dimensional quantum system (a qubit), i.e., $\mathcal{H}_{(i)_{(i-1)}} \cong \mathcal{H}_{(i)_{(i+1)}} \cong \mathbb{C}^2$, for all $i \in V$. We then encode the quantum walk state $|(i,i-1),i\rangle$ with the automaton state $|\dots, (0,0)_{i-1}, (1_{i-1}, 0_{i+1})_i, (0,0)_{i+1}, \dots\rangle$, while the state $|(i,i+1),i\rangle$ is written as $|\dots, (0,0)_{i-1}, (0_{i-1}, 1_{i+1})_i, (0,0)_{i+1}, \dots\rangle$. In this way, an excited subcell (a qubit in the 1 state) indicates the walker position and its movement direction. All the encoding is done within the single excitation subspace.

For the dynamics translation, for clarity, we will employ one tiling for each quantum walk unitary. As such, we require three tilings. The first one, \mathcal{T}_0 , is related to the coin operator. As this only changes the edge state, without moving the walker, the tiles are the very subcells of each cell: $T_i^{(0)} = \{(i)_{i-1}, (i)_{i+1}\}$. The unitary W_0 associated to this tiling is of the same form as the unitary C_i employed in the coin C :

$$W_0 = \begin{pmatrix} 1 & 0 & 0 & 0 \\ 0 & q & p & 0 \\ 0 & p & q & 0 \\ 0 & 0 & 0 & 1 \end{pmatrix},$$

also fulfilling the requirements that $|p|^2 + |q|^2 = 1$ and $p^*q + q^*p = 0$. Note that now such operator

acts on a two-qubit system, $W_0 : \mathcal{H}_{\Sigma_{(i,i-1)}} \otimes \mathcal{H}_{\Sigma_{(i,i+1)}} \rightarrow \mathcal{H}_{\Sigma_{(i,i-1)}} \otimes \mathcal{H}_{\Sigma_{(i,i+1)}}$, and it is written in the basis $\{|(0,0)_i\rangle, |(0,1)_i\rangle, |(1,0)_i\rangle, |(1,1)_i\rangle\}$. Moreover, notice that W_0 only acts non-trivially on the single excitation subspace. Writing a general state $|\Psi(t)\rangle$ for the automaton at time t as:

$$\sum_{i \in \mathbb{Z}} \left[\Psi_{(i,i-1)}(i,t) |\dots, (0,0)_{i-1}, (1_{i-1}, 0_{i+1})_i, (0,0)_{i+1}, \dots\rangle + \Psi_{(i,i+1)}(i,t) |\dots, (0,0)_{i-1}, (0_{i-1}, 1_{i+1})_i, (0,0)_{i+1}, \dots\rangle \right],$$

where $\Psi_{(i,\pm 1)}(i,t)$ is the probability amplitude of finding an “excitation” at the subcell $i \pm 1$ of the i -th cell at time t , after the evolution corresponding to the first tiling,

$\left(\bigotimes_{T_j^{(0)} \in \mathcal{T}_0} W_0 \right) |\Psi(t)\rangle$, we get:

$$\sum_{i \in \mathbb{Z}} \left[\Psi_{(i,i-1)}(i,t) |\dots, (0,0)_{i-1}, (q_{i-1}, p_{i+1})_i, (0,0)_{i+1}, \dots\rangle + \Psi_{(i,i+1)}(i,t) |\dots, (0,0)_{i-1}, (p_{i-1}, q_{i+1})_i, (0,0)_{i+1}, \dots\rangle \right].$$

Now we use a second tiling \mathcal{T}_1 , to simulate the flip-flop shift operator S_I . The second tiling is thus responsible for the interaction between the cells. As such, the associated unitary operation W_1 must act on tiles that contain subcells from neighboring cells. As the walker wave-function can only spread by one vertex in a single step, to the left and to the right, the automaton neighborhood is given by $\mathcal{N} = \{j-1, j, j+1\}$. From the definition of the flip-flop shift operator S_I and the encoding of the coin-walker state in the automaton language, we note that the probability amplitude in the subcell $i+1$ of the i -th cell $(i)_{i+1}$ is to be transferred to the subcell i of the $(i+1)$ -th cell $((i+1)_i)$, and vice-versa – in the graph perspective, we create an edge $(i, i+1)$ for all V . Given that, for the tiling \mathcal{T}_1 we set the tiles $T_i^{(1)} = \{(i)_{i+1}, (i+1)_i\}$, and the unitary function W_1 is simply the SWAP operator. After the evolution due to these two tilings, $\left(\bigotimes_{T_j^{(1)} \in \mathcal{T}_1} W_1 \right) \left(\bigotimes_{T_j^{(0)} \in \mathcal{T}_0} W_0 \right)$, a general state $|\Psi(t)\rangle$ the state of the automaton reads:

$$\sum_{i \in V} \left[\Psi_{(i,i-1)}(i,t) |\dots, (0_{i-2}, q_i)_{i-1}, (0,0)_i, (p_i, 0_{i+2})_{i+1}, \dots\rangle + \Psi_{(i,i+1)}(i,t) |\dots, (0_{i-2}, p_i)_{i-1}, (0,0)_i, (q_i, 0_{i+2})_{i+1}, \dots\rangle \right].$$

Lastly, we need to simulate the action of the X operator with a third tiling, \mathcal{T}_2 . Like for the coin operator, the X operator does not change the walker’s position. As such, its corresponding operator acts only on individual cells: $T_i^{(2)} = \{(i)_{i-1}, (i)_{i+1}\}$. Moreover, as the action of each X_i is simply to change the movement direction, here we only need to take W_2 as a SWAP operator acting in each cell to get:

$$\sum_{i \in V} \left[\Psi_{(i,i-1)}(i,t) |\dots, (q_{i-2}, 0_i)_{i-1}, (0,0)_i, (0_i, p_{i+2})_{i+1}, \dots\rangle + \Psi_{(i,i+1)}(i,t) |\dots, (p_{i-2}, 0_i)_{i-1}, (0,0)_i, (0_i, q_{i+2})_{i+1}, \dots\rangle \right].$$

That is the automaton state after on time step, i.e., after the action of $\mathcal{E} =$

$$\left(\bigotimes_{T_j^{(2)} \in \mathcal{T}_2} W_2\right) \left(\bigotimes_{T_j^{(1)} \in \mathcal{T}_1} W_1\right) \left(\bigotimes_{T_j^{(0)} \in \mathcal{T}_0} W_0\right).$$

It is now immediate to obtain the recurrence relations that describe the automaton dynamics:

$$\begin{aligned}\Psi_{(i-2,i-1)}(i-1,t+1) &= q\Psi_{(i,i-1)}(i,t) + p\Psi_{(i,i+1)}(i,t), \\ \Psi_{(i+2,i+1)}(i+1,t+1) &= p\Psi_{(i,i-1)}(i,t) + q\Psi_{(i,i+1)}(i,t).\end{aligned}$$

These are exactly the same recurrence relations for the 1-d coined quantum walk. Both dynamics are thus identical at every time-step.

3. General Recipe

Now we give a prescription to find the QCA correspondent to a given coined QW on a d -regular graph. As input we take a d -regular graph $G = G(E, V)$ (or lattice L) where the quantum walk is defined; the coin operator C ; and the shift operator S_π . As output we must return a complete PUQCA whose evolution is the same as the CQW. The steps to find this translation are enumerated below.

1. The number of cells in the automaton is given the number of vertices, $|V|$, of the graph G . As the graph is d -regular, each cell is split in d subcells. We place one qubit in each subcell, and then a total of $|V|.d$ qubits are employed (see the resources discussion below).
2. The automaton neighborhood scheme \mathcal{N} is determined by the graph-neighborhood \mathcal{N}^G , by the simple inclusion of the “central” cell: $\mathcal{N}_i = \mathcal{N}_i^G \cup \{i\}$.
3. To each CQW_d state $|(i, j), i\rangle$ we associate the automaton (single excitation subspace) state $|\dots(0_h, \dots, 1_j, \dots, 0_m)_{i\dots}\rangle$, where h, m and all other subindex labeling the subcells of cell i belong to \mathcal{N}_i^G . While the subindex i gives us in which cell the excitation is located, the subindex j tells us its subcell location (corresponding to the movement direction). In this way the space associated to each cell is $\mathcal{H}_\Xi = (\mathbb{C}^2)^{\otimes d}$.
4. To simulate the CQW_d dynamics within the automata language three tilings are sufficient [38]. The first tiling is related to the action of the coin, with each tile given by all subcells that belongs to the same cell: $T_i^{(0)} = \{(i)_j | j \in \mathcal{N}_i^G\}$. The second tiling is devoted to the simulation of the flip-flop shift acting on neighboring cells. From the definition of S_I we can see that in terms of QCA we have the subcell j in the cell i interacting with the

subcell i of the j -th cell, and vice-versa. Therefore $T_{(i,j)}^{(1)} = \{(i)_j, (j)_i\}$ where $(i, j) \in E$. The third tiling is responsible for simulating the permutation that connects S_I to S_π . As this operation is “local” in each vertex, then $T_i^{(1)} = \{(i)_j | j \in \mathcal{N}_i^G\}$.

5. To each tiling we associate one unitary operator. To the first tiling, the unitary operator $W_0 : \mathcal{H}_\Xi \rightarrow \mathcal{H}_\Xi$ is directly related to the unitary operator C_i by employing the unary representation for the cell states (see two steps above) within the single excitation subspace. Out of this subspace the action of W_0 is trivial, being completed by ones in the diagonal entries. Since the flip-flop operator is translated as a swap between the two subcells of neighboring cells, the unitary $W_1 : \mathcal{H}_{(i)_j} \otimes \mathcal{H}_{(j)_i} \rightarrow \mathcal{H}_{(i)_j} \otimes \mathcal{H}_{(j)_i}$, for $(i, j) \in E$, is the SWAP gate between them. Lastly, $W_2 : \mathcal{H}_\Xi \rightarrow \mathcal{H}_\Xi$ implements the permutation π on the cell i , by encoding the operator π_i in the same way as for the coin operator.

These steps give the full translation between a CQW_d and a QCA.

Before we move on, we compare the resources required in each model. The dimension of the Hilbert space in the quantum walk model is $2|E|$, which is equal $|V|.d$ due to the assumed d -regularity of the graph. For the corresponding QCA at first sight we would need a Hilbert space of dimension $|V|.2^d$. Nevertheless, as we only need the single excitation subspace for our construction, whose dimension is d , we in fact only use an effective Hilbert space with dimension $|V|.d$. Therefore, both models require the same amount of resources.

B. SQWH \subseteq QCA

Sometime after the development of the coined quantum walk model, it was realized that similar coherent dynamics could be obtained even without a coin space. In such models the coin is removed and the walker’s dispersion over a graph is obtained via the alternation of operators directly acting on the walker’s position space. The first “coinless” quantum walk model was proposed by Szegedy [39], followed by the staggered quantum walk [11, 12, 40, 41], and, more recently, by the staggered quantum walks with Hamiltonians (SQWH) [12]. The latter was shown to encompass the previous two models of coinless quantum walks, and even some coined models [12]. Furthermore, the SQWH has been shown to be useful for quantum search [42],

and an experimental proposal is already in place [43]. Our aim here is thus to show that the PUQCA can simulate the SQWH, and with that inherit the simulation of various coinless, and coined, models.

We start by describing the SQWH over a graph $G = G(V, E)$ [12]. As before, to each vertex $i \in V$ we associate a unit vector $|i\rangle$, with $\langle i|j\rangle = \delta_{ij}$ for all $i, j \in V$. As such, to the vertices of G we associate the Hilbert space $\mathcal{H}_V = \text{span}(\{|i\rangle \mid i \in V\})$. Crucial to the SQWH is the concept of a graph *tessellation*: A graph tessellation \mathfrak{T} is a partition of the graph into complete subgraphs, i.e., into cliques. Such a partition directly induces a partition of \mathcal{H}_V : let α be an element of \mathfrak{T} , then $\mathcal{H}_\alpha = \bigoplus_{i \in \alpha} \mathcal{H}_i$, where $\mathcal{H}_i = \text{span}(\{|i\rangle \mid i \in \alpha\})$. Each element α is called a polygon, as it is related to a clique. It is now simple to define a rank-one projector $|\alpha\rangle\langle\alpha|$ into \mathcal{H}_α , by defining the vector

$$|\alpha\rangle = \sum_{i \in \alpha} a(i) |i\rangle,$$

where $a(i) \in \mathbb{C}$ and $\sum_{i \in \alpha} |a(i)|^2 = 1$. Note that the coefficients a do not depend on the polygon in a given tessellation, but they do depend on the label given to each vertex within polygon [12]. A dynamics that does not connect different subspaces \mathcal{H}_α can be given by the Hamiltonian operator associated with this tessellation as

$$H_{\mathfrak{T}} = 2 \sum_{\alpha \in \mathfrak{T}} |\alpha\rangle\langle\alpha| - \mathbb{1}. \quad (7)$$

Such operator is known as the orthogonal reflection of the graph [41], and it is Hermitian and unitary, implying that $H_{\mathfrak{T}}^2 = \mathbb{1}$. The dynamics generated by this Hamiltonian is then $U_{\mathfrak{T}} = \exp(i\theta H_{\mathfrak{T}})$, with $\theta \in [0, 2\pi]$. This propagator respects the partition of \mathcal{H}_V into subspaces related to the tessellation polygons, as $U_{\mathfrak{T}} = \bigoplus_{\alpha \in \mathfrak{T}} U_\alpha$ with

$$U_\alpha = e^{-i\theta} \mathbb{1}_\alpha + 2i \sin(\theta) \sum_{i, j \in \alpha} a^*(i) a(j) |i\rangle\langle j|; \quad (8)$$

where $\mathbb{1}_\alpha := \sum_{i \in \alpha} |i\rangle\langle i|$ is the identity operator in the α subspace.

If the dynamics of the walker was to be given simply by the propagator $U_{\mathfrak{T}}$, then a walker starting in a vertex $i \in V$ would remain stuck in the polygon that contains such a vertex. As Szegedy noticed [39], a walker dispersion over a graph can be obtained without a coin if we alternate propagation operators, with each of them acting within a different subspace-partition of \mathcal{H}_V . At this point we observe that a given tessellation contains all the vertices of a graph, but not necessarily all its edges. In [12] it was defined a set of tessellations, a *tessellation cover* $\{\mathfrak{T}_0, \dots, \mathfrak{T}_{N-1}\}$, whose union also covers the edge

set. Each tessellation \mathfrak{T}_k induces a different subspace-partition of \mathcal{H}_V , with associated Hamiltonian $H_{\mathfrak{T}_k}$ constructed in the same way as in Eq.(7). One time-step evolution of the SQWH is then generated by the operator

$$U = \prod_{k=0}^{N-1} e^{i\theta_k H_{\mathfrak{T}_k}} \quad (9)$$

with $\theta_k \in [0, 2\pi]$ for all $k \in \{0, \dots, N-1\}$.

We are now ready to show how to translate the SQWH model into a QCA one. As previously, before giving a general recipe we first show a simple example of such translation.

1. One dimensional example

In this example, we consider a SQWH over a 1-d lattice. The vertex set is $V = \mathbb{Z}$, and thus $\mathcal{H}_V = \text{span}(\{|i\rangle \mid i \in \mathbb{Z}\})$. The smallest tessellation cover for such 2-regular (infinite) graph is composed of two tessellations $\{\mathfrak{T}_0, \mathfrak{T}_1\}$, with $\mathfrak{T}_0 = \{\bullet \xrightarrow{2i} \bullet \xrightarrow{2i+1} \bullet \mid i \in \mathbb{Z}\}$ and $\mathfrak{T}_1 = \{\bullet \xrightarrow{2i+1} \bullet \xrightarrow{2i+2} \bullet \mid i \in \mathbb{Z}\}$. These tessellations are shown Fig.(3). Each tessellation induces a different partition of \mathcal{H}_V as $\bigoplus_{\alpha_k \in \mathfrak{T}_k} \mathcal{H}_{\alpha_k}$, with $k \in \{0, 1\}$. For this example we take general projectors into each polygon-subspace via the vectors

$$\begin{aligned} |\bullet \xrightarrow{2i} \bullet \xrightarrow{2i+1} \bullet\rangle &= a_0 |2i\rangle + \tilde{a}_0 |2i+1\rangle, \\ |\bullet \xrightarrow{2i+1} \bullet \xrightarrow{2i+2} \bullet\rangle &= a_1 |2i+1\rangle + \tilde{a}_1 |2i+2\rangle, \end{aligned}$$

for all $i \in \mathbb{Z}$, and where the coefficients are constrained to $|a_k|^2 + |\tilde{a}_k|^2 = 1$ with $k \in \{0, 1\}$. With these projectors we follow Eq.(7) to construct the evolution operator as

$$U = e^{i\theta_1 H_{\mathfrak{T}_1}} e^{i\theta_0 H_{\mathfrak{T}_0}}.$$

As the evolution propagator is composed by the product of similar operators, $e^{i\theta_k H_{\mathfrak{T}_k}}$, acting in similar ways in different partitions of \mathcal{H}_V , below we only show how to translate a single of these operators, say $e^{i\theta_0 H_{\mathfrak{T}_0}}$, into automata language. Still within the SQWH language, with the aid of Eq.(8), the propagator in each subspace is

$$\begin{aligned} U_{\bullet \xrightarrow{2i} \bullet \xrightarrow{2i+1} \bullet} &= e^{-i\theta_0} \left(|2i\rangle\langle 2i| + |2i+1\rangle\langle 2i+1| \right) + \\ & 2i \sin(\theta_0) \left(|a_0|^2 |2i\rangle\langle 2i| + a_0^* \tilde{a}_0 |2i\rangle\langle 2i+1| + \right. \\ & \left. a_0 \tilde{a}_0^* |2i+1\rangle\langle 2i| + |\tilde{a}_0|^2 |2i+1\rangle\langle 2i+1| \right). \end{aligned}$$

The evolution operator for this tessellation is then $U_{\mathfrak{T}_0} = \bigoplus_{i \in \mathbb{Z}} U_{\bullet \xrightarrow{2i} \bullet \xrightarrow{2i+1} \bullet}$. Let a general walker state at time t be expressed as $|\psi(t)\rangle = \sum_{i \in \mathbb{Z}} \psi(i, t) |i\rangle$, where $\psi(i, t)$ is the

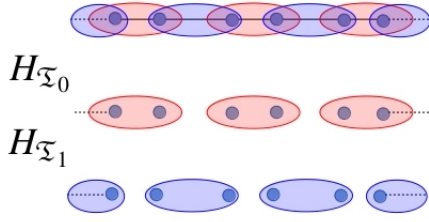


FIG. 3. This picture shows the two tessellations used in the 1-d example of translation between the SQWH and the PUQCA. Within the SQWH the operator U_0 (U_1) acts on the red (blue) polygons. In the PUQCA picture, this is translated to the action of W_0 (W_1) on the qubits in the red (blue) tiles.

probability amplitude for vertex i at time t . The state after the action of $U_{\mathfrak{T}_0}$ is then given by

$$U_{\mathfrak{T}_0} |\psi(t)\rangle = \sum_{i \in \mathbb{Z}} \left\{ [(e^{-i\theta_0} + 2i \sin(\theta_0) |a_0|^2) \psi(2i, t) + 2i \sin(\theta_0) a_0 \tilde{a}_0^* \psi(2i+1, t)] |2i\rangle + [(e^{-i\theta_0} + 2i \sin(\theta_0) |\tilde{a}_0|^2) \psi(2i+1, t) + 2i \sin(\theta_0) \tilde{a}_0 a_0^* \psi(2i, t)] |2i+1\rangle \right\}. \quad (10)$$

This is the evolution that we want to simulate within the quantum cellular automata model.

For the QCA simulation, in each lattice vertex we place one qubit. The two tessellations needed for the walker dynamics will now give us two tilings. The polygons of the first tessellation determine now the tiles of the first tiling: $T_i^{(0)} = \{2i, 2i+1\}$. Similarly, for the second tiling the correspondence implies the tiles $T_i^{(1)} = \{2i+1, 2i+2\}$. There are two possibilities to define the cellular automaton cell: first is to take the tiles of the first tiling as forming a single cell with two subcells; second is to consider each vertex as a single cell with no subcell division. Both cases are equivalent, and we take the second choice as it simplifies the simulation description. The encoding of the walker state into the QCA framework is then simply given by $|i\rangle \rightarrow |\dots, 0_{i-1}, 1_i, 0_{i+1}, \dots\rangle$, for all $i \in V$. A general state for the automaton at time t is then written as $|\Psi(t)\rangle = \sum_{i \in \mathbb{Z}} \Psi(i, t) |\dots, 0_{i-1}, 1_i, 0_{i+1}, \dots\rangle$, with $\Psi(i, t)$ the amplitude of finding an “excitation” at the i -th qubit at time t . Now we need to simulate the evolution operator $U_{\mathfrak{T}_0}$ with the action of the first tiling. To that we note that each polygon in \mathfrak{T}_0 corresponds exactly to a tile in \mathcal{T}_0 . Therefore, the propagator $U_{\mathfrak{T}_0} =$

$\bigoplus_{\alpha_0 \in \mathfrak{T}_0} U_{\alpha_0}$ is then translated into $\bigotimes_{T_i^{(0)} \in \mathcal{T}_0} W_0$, where

$$W_0 = \begin{pmatrix} 1 & 0 & 0 & 0 \\ 0 & e^{-i\theta_0} + 2i \sin(\theta_0) |a_0|^2 & 2i \sin(\theta_0) a_0 \tilde{a}_0^* & 0 \\ 0 & 2i \sin(\theta_0) a_0^* \tilde{a}_0 & e^{-i\theta_0} + 2i \sin(\theta_0) |\tilde{a}_0|^2 & 0 \\ 0 & 0 & 0 & 1 \end{pmatrix},$$

when written in the computational basis $\{|0_{2i}, 0_{2i+1}\rangle, |0_{2i}, 1_{2i+1}\rangle, |1_{2i}, 0_{2i+1}\rangle, |1_{2i}, 1_{2i+1}\rangle\}$. With such an encoding, the evolution given by $\bigotimes_{T_i^{(0)} \in \mathcal{T}_0} W_0$ leads a general state of the automaton at time t to the state:

$$\sum_{i \in \mathbb{Z}} \left\{ [(e^{-i\theta_0} + 2i \sin(\theta_0) |a_0|^2) \Psi(2i, t) + 2i \sin(\theta_0) a_0 \tilde{a}_0^* \Psi(2i+1, t)] |\dots, 0_{2i-1}, 1_{2i}, 0_{2i+1}, 0_{2i+2}, \dots\rangle + [(e^{-i\theta_0} + 2i \sin(\theta_0) |\tilde{a}_0|^2) \Psi(2i+1, t) + 2i \sin(\theta_0) \tilde{a}_0 a_0^* \Psi(2i, t)] |\dots, 0_{2i-1}, 0_{2i}, 1_{2i+1}, 0_{2i+2}, \dots\rangle \right\}. \quad (11)$$

After decoding, this state is exactly equivalent to the SQWH state shown in Eq.(10).

This example shows that the tessellations in the SQWH play the role of the tilings in the QCA, and the set of operators $\{W_i\}$ in the QCA are obtained from the polygon-subspace operators associated with the tessellations of the SQWH.

C. General Recipe

The general procedure to translate a SQWH into a PUQCA takes as input a d -regular graph $G = G(E, V)$ (or lattice L), a tessellation cover $\{\mathfrak{T}_k\}_{k=0}^{N-1}$ with polygons α_k for each tessellation, a set of coefficients $\{a_k(i)\}_{i=0}^{|\alpha_k|-1}$, and a set of angles $\{\theta_k\}_{k=0}^{N-1}$. As result, the procedure outputs a well-formed PUQCA by following the subsequent recipe.

1. The PUQCA is established over the same graph G employed by the SQWH.
2. Since the graph is the same, the neighborhood scheme for the corresponding automaton is simply $\mathcal{N}_i = \{j | (i, j) \in E\} \cup \{i\}$.
3. No subcell structure is required for this translation ($n = 0$). In each vertex we place a qubit, and thus $\mathcal{H}_{\Xi} \cong \mathbb{C}^2$. To each vertex state $|i\rangle$ on the SQWH side, we associate the automaton state $|\dots, 0_{i-1}, 1_i, 0_{i+1}, \dots\rangle \in \mathcal{H}_{\Xi}^{\otimes |V|}$.
4. For each tessellation \mathfrak{T}_k for the SQWH, we have an equivalent tiling \mathcal{T}_k in the PUQCA. Moreover,

the vertices belonging to the polygon α_k of the k -th tessellation yield the elements of the tile $T_k^{(i)}$.

5. With the input data, following the prescription of the SQWH, we construct the evolution operator $U_{\mathfrak{T}_k} = \bigoplus_{\alpha_k \in \mathfrak{T}_k} U_{\alpha_k}$ to each tessellation. As the polygons α_k are all identical for a d -regular graph, the operators U_{α_k} , acting in each polygon-subspace are also identical. Such operator is then directly translated to the PUQCA model as the unitary function W_k , via the unary encoding described in the item 3 above.

This completes the translation from the SQWH to the PUQCA model. As we have done before, let us analyze the resources required by the PUQCA formalism for a given a SQWH dynamics. For a graph $G = G(E, V)$, the Hilbert space associated with the SQWH is a $|V|$ -dimensional one. For the PUQCA we employed $|V|$ qubits, yielding a $2^{|V|}$ -dimensional total space. However, here again, we only use the single-excitation subspace, which is $|V|$ -dimensional. Once more, the effective amount of resources required by the PUQCA are the same as the original model.

IV. DISCUSSION AND CONCLUSIONS

In this work we introduced a partitioned quantum cellular automata, the PUQCA, which is at the same time a well-formed quantum cellular automata, and also a conceptually simple and versatile construction. Such characteristics allowed us to show that various models of quantum walks can be readily translated into a PUQCA dynamics. This has the immediate advantage to employ qubits, the most common basic architecture of quantum computers. As such it is more convenient for near term experimental implementations of, for instance, quantum search algorithms. It is important to notice that the translation from quantum walk models to quantum cellular automata proposed here requires the same amount of effective dimensions.

One question that immediately raises from our translation results ($QW \rightarrow QCA$) is whether quantum walks and

quantum cellular automata are equivalent, i.e., if there is for every QCA an correspondent QW ($QW \leftarrow QCA$). Of course this depends on how strict the definitions of the models are. For instance, it is usually accepted that in a coined quantum walk, the shift operator does not create superposition of the walker's position states. When translating CWQ into PUQCA, this implied that all the interactions between cells were simply SWAP gates. Therefore, if a given PUQCA has an interaction between cells other than a SWAP gate, our results suggest that there is no equivalent coined quantum walk to such a PUQCA. Another interesting perspective of our work is to allow for comparing different types of resources across different models. We can compare, for example, how the coherence created within the staggered quantum walk models is translated into entanglement between qubits in the quantum cellular automata model.

To conclude, we recall that the idea of quantum computers was arguably created by Feynman as a way (possibly the only one) to simulate complex quantum systems. In his seminal article entitled "Simulating Physics with Computers" [44], he constructs the idea of a simulator of physical systems from the idea of a cellular automata. At that time quantum cellular automata were not yet invented. From there on, various definitions of QCA were developed, but the potential of quantum cellular automata models as simulators of complex quantum systems remains largely unexplored. We hope that our first results in this direction, together with a simple formulation of a QCA model and its possibility of implementation with current technology, will serve as the catalyst for the development of a whole new phenomenology of simulation of quantum systems.

ACKNOWLEDGMENTS

We would like to thank Osvaldo J. Farias for various discussions on the topic of quantum cellular automata. We acknowledge financial support from the National Institute for Science and Technology of Quantum Information (INCT-IQ/CNPq, Brazil).

[1] Frank Spitzer. *Principles of Random Walk*. Springer Science+Business Media, LLC, second edition, 1976.
[2] Vijay Singal. *Beyond the Random Walk*. Oxford, 2004.
[3] Robert J. Shiller and Pierre Perron. Testing the random walk hypothesis: Power versus frequency of observation. *Economics Letters*, 18:381–386, 1985.

[4] Francois Fouss, Alain Pirotte, Jean-Michel Renders, and Marco Saerens. Random-walk computation of similarities between nodes of a graph with application to collaborative recommendation. *IEEE Transactions on Knowledge and Data Engineering*, 19(3), March 2007.
[5] Fugao Wang and D. P. Landau. Efficient, multiple-range random walk algorithm to calculate the density of states.

- Physical Review Letters*, 86:2050–2053, March 2001.
- [6] Wiersma and Diederik S. The physics and applications of random lasers. *Nature Physics*, 4:359–367, May 2008.
 - [7] Y. Aharonov, L. Davidovich, and N. Zagury. Quantum random walks. *Physical Review A*, pages 1687–1690, August 1993.
 - [8] G Di Molfetta and A Pérez. Quantum walks as simulators of neutrino oscillations in a vacuum and matter. *New Journal of Physics*, 18, October 2016.
 - [9] Pablo Arrighi, Stefano Facchini, and Marcelo Forets. Quantum walking in curved spacetime. *Quantum Information Processing*, 15:3467–3486, May 2016.
 - [10] Renato Portugal. *Quantum Walks and Search Algorithm*. Springer, 2013.
 - [11] R. Portugal, R.A.M. Santos, T.D. Fernandes, and D. N. Gonçalves. The staggered quantum walk model. *Quantum Information Processing*, 15:85–101, January 2016.
 - [12] R. Portugal, M. C. de Oliveira, and J. K. Moqadam. Staggered quantum walks with hamiltonians. *Physical Review A*, 2017.
 - [13] Andrew M Childs. Universal computation by quantum walk. *Physical Review Letters*, 102:4, May 2009.
 - [14] Andrew M. Childs, David Gosset, and Zak Webb. Universal computation by multi-particle quantum walk. *Science*, 339:791–794, 2013.
 - [15] F. Zähringer, G. Kirchmair, R. Gerritsma, E. Solano, R. Blatt, and C. F. Roos. Realization of a quantum walk with one and two trapped ions. *Physical Review Letters*, 104:100503, 2010.
 - [16] R. Raussendorf W. Dür, V. M. Kendon, and H.-J. Briegel. Quantum walks in optical lattices. *Physical Review A*, 66:052319, November 2002.
 - [17] Kia ManouchehriJingbo Wang. *Physical Implementation of Quantum Walks*. Springer, 2013.
 - [18] Bastien Chopard and Michel Droz. *Cellular Automata Modeling of Physical Systems*. Cambridge University Press, 2005.
 - [19] S. Wolfram. *A new kind of science*. Wolfram Media, 2002.
 - [20] John von Neumann. *Theory of Self-Reproducing Automata*. University of Illinois Press, 1996.
 - [21] S. Nandi, B. K. Kar, and P. Pal Chaudhuri. Theory and applications of cellular automata in cryptography. *IEEE Transactions on Computers*, 43(12), December 1994.
 - [22] U. Frisch, B. Hasslacher, and Y. Pomeau. Lattice gas automata for the navier-stokes equation. *Physical Review Letters*, 56(14), 1986.
 - [23] D. G. Green. Cellular automata models in biology. *Mathematical and Computer Modelling*, 1990.
 - [24] Gerhard Grossing and Anton Zeilinger. Quantum cellular automata. *Complex Systems*, 2:197–208, 1988.
 - [25] David A. Meyer. From quantum cellular automata to quantum lattice gases. *Journal of Statistical Physics*, 85:551–574, December 1996.
 - [26] Karoline Wiesner. Quantum cellular automata. *arXiv:0808.0679v1 [quant-ph]*, 2008.
 - [27] Pablo Arrighi and Jonathan Grattage. Partitioned quantum cellular automata are intrinsically universal. *Natural Computing*, 11:13–22, March 2012.
 - [28] S. et al Boixo. Evidence for quantum annealing with more than one hundred qubits. *Nature Physics*, 10:218–224, 2014.
 - [29] Abhinav Kandalar and S. et al. Hardware-efficient quantum optimizer for small molecules and quantum magnets. *arXiv:1704.05018v1 [quant-ph]*, 2017.
 - [30] John M. Martinis and S. et al. Qubit compatible superconducting interconnects. *arXiv:1708.04270 [quant-ph]*, 2017.
 - [31] Göran Lindblad. A general no-cloning theorem. *Letters in Mathematical Physics*, 47:189–196, 1999.
 - [32] T. Toffoli and N. Margolus. *Cellular Automata Machines*. MIT Press Series in Scientific Computation, 1987.
 - [33] Carlos A., Perez Delgado, and Donny Cheung. Local unitary quantum cellular automata. *Physical Review A*, 76(032320), 2007.
 - [34] J.Watrous. On one-dimensional quantum cellular automata. In *Proceedings of the 36th Symposium on Foundations of Computer Science*, pages 528–537, 1995.
 - [35] Pascal Philipp and Renato Portugal. Exact simulation of coined quantum walks with the continuous-time model. *Quantum Information Processing*, 2016.
 - [36] Note that the space \mathcal{H}_G is not given by the tensor product of a space associated to the edges and another space associated to the vertices.
 - [37] Note that since the evolution for t time steps is given by U^t , then the operator X can be absorbed in the coin operator by suitably applying corrections on the initial and final state: $U^t = X \cdot (S_I \cdot CX)^t X^{-1}$.
 - [38] Here again the action of the third tiling can be absorbed in the action of the first one, plus modifications in the initial and final state. We however present the translation with three tilings for clarity reasons.
 - [39] M. Szegedy. Quantum speed-up of markov chain based algorithms. In *Proceedings of the 45th Symposium on Foundations of Computer Science*, pages 32–41, 2004.
 - [40] Renato Portugal, Stefan Boettcher, and Stefan Falkner. One-dimensional coinless quantum walks. *Phys. Rev. A*, 91:052319, May 2015.
 - [41] Renato Portugal. Staggered quantum walks on graphs. *Phys. Rev. A*, 2016.
 - [42] R. Portugal and T. D. Fernandes. Quantum search on the two-dimensional lattice using the staggered model with hamiltonians. *Phys. Rev. A*, 95:042341, Apr 2017.
 - [43] J. Khatibi Moqadam, M. C. de Oliveira, and R. Portugal. Staggered quantum walks with superconducting microwave resonators. *Phys. Rev. B*, 95:144506, Apr 2017.
 - [44] R.P.Feynman. Simulating physics with computers. *Int. J. of Theor. Phys.*, 1982.